

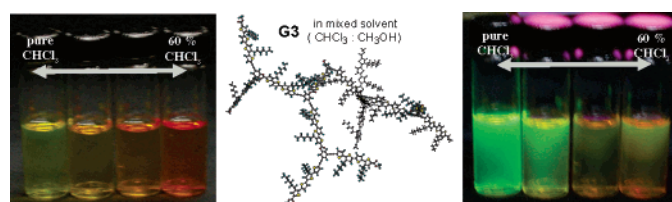
Synthesis, Optical, and Electrochemical Properties of a New Family of Dendritic Oligothiophenes

Yong Zhang,[‡] Chunchang Zhao,[†] Jinhua Yang,[†] Mbiya Kapiamba,[†] Olesya Haze,[†] Lewis J. Rothberg,^{*,†,‡} and Man-Kit Ng^{*,†}

Department of Chemistry, and Department of Chemical Engineering, University of Rochester, Rochester, New York 14627

rothberg@chem.rochester.edu; ng@chem.rochester.edu

Received September 21, 2006



A new class of semi-flexible dendrimers with oligothiophene (OT) arms up to the third generation have been synthesized and investigated. The synthetic methods employed include a combination of palladium-catalyzed Stille cross-coupling reactions for oligothiophenes, Sonogashira cross-coupling reactions for building blocks, and carbodiimide-mediated esterification for building up the various dendrimers. The optical and electrochemical properties of this series of oligothiophenes-based dendrimers are shown to be strongly influenced by their morphologies as demonstrated by their pronounced solvatochromic and thermochromic responses under different environmental conditions. Introducing rigid oligothiophene arms to shape non-persistent ester-linked dendrimers causes higher generation dendrimers (**G2** and **G3**) to exhibit solvatochromism and thermochromism, while their oligomeric counterpart (**3b**) and lower generation (**G1**) analogue do not. Spectroscopic changes due to both intramolecular and intermolecular aggregations are observed.

Introduction

Dendrimers have a regular, highly branched, monodispersed, and treelike globular architecture that differentiates them from linear, branched, or cross-linked polymers and endows them with distinct chemical, physical, and functional properties.¹ Dendrimers can be characterized by whether the linking unit renders them flexible (“shape non-persistent”) or rigid (“shape persistent”). Most of the Fréchet-type, ester- and amide-based dendrimers are essentially flexible due to the presence of benzylic ether, ester, or amide linkages that are conveniently accessible by classical synthetic methodologies, including but not limited to the Williamson ether synthesis, polyester, and

polyamide synthesis.² These dendritic macromolecules have been widely investigated for catalytic and therapeutic applications because of their solubility, flexibility, and biocompatibility.³ On the other end of the spectrum, Moore and co-workers designed a series of phenylacetylene-based dendrimers and developed the concept of “shape persistent” dendrimers associated with rigid, conjugated backbones.^{4a,b} These molecules combined many useful properties of dendrimers such as uniformity and processability with those of semiconducting conjugated materials such as charge transport and strong luminescence efficiency.⁴

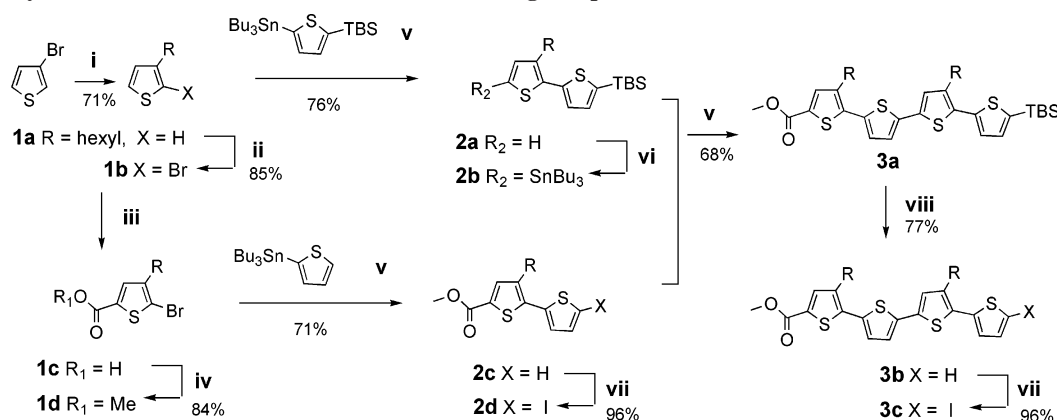
One of most investigated families of conjugated molecules is the oligo- and polythiophenes, which have attracted intense interest for applications in many promising organic electronic

[†] Department of Chemistry.

[‡] Department of Chemical Engineering.

(1) (a) Fréchet, J. M. J. *Science* **1994**, *263*, 1710–1715. (b) Jansen, J. F. G. A.; de Brabander-van, den Berg, E. M. M.; Meijer, E. W. *Science* **1994**, *266*, 1226–1229. (c) Newkome, G. R.; Moorefield, C. N.; Vögtle, F. *Dendritic Molecules: Concepts, Syntheses, Perspectives*; Wiley: Weinheim, 1996. (d) Zeng, F.; Zimmerman, S. C. *Chem. Rev.* **1997**, *97*, 1681–1712. (e) Fréchet, J. M. J. *J. Polym. Sci., Part A: Polym. Chem.* **2003**, *41*, 3713–3725. (f) Pyun, J.; Zhou, X.-Z.; Drockenmuller, E.; Hawker, C. J. *J. Mater. Chem.* **2003**, *13*, 2653–2660.

(2) (a) Hawker, C. J.; Fréchet, J. M. J. *J. Am. Chem. Soc.* **1990**, *112*, 7638–7647. (b) Nummelin, S.; Skrifvars, M.; Rissanen, K. *Top. Curr. Chem.* **2000**, *210*, 1–65. (c) Gilat, S. L.; Adronov, A.; Fréchet, J. M. J. *Angew. Chem., Int. Ed.* **1999**, *38*, 1422–1427. (d) Ihre, H.; Padilla, De Jesús, O. L.; Fréchet, J. M. J. *J. Am. Chem. Soc.* **2001**, *123*, 5908–5917. (e) Morgan, M. T.; Carnahan, M. A.; Immoos, C. E.; Ribeiro, A. A.; Finkelstein, S.; Lee, S. J.; Grinstaff, M. W. *J. Am. Chem. Soc.* **2003**, *125*, 15485–15489.

SCHEME 1. Synthetic Routes for Dimeric and Tetrameric Oligothiophenes 2a–d and 3a–c^a

^a Reagents and conditions: (i) C₆H₁₃MgBr, 0.12 mol % Ni(dppp)Cl₂, Et₂O, reflux; (ii) NBS, CHCl₃/HOAc, rt; (iii) (1) LDA, THF, 0 °C; (2) dry ice (CO₂), −78 °C; (iv) MeOH, cat. H₂SO₄, reflux; (v) 0.5 mol % Pd(PPh₃)₂Cl₂, 1 mol % PPh₃, DMF, 110 °C; (vi) (1) *n*-BuLi, THF, 0 °C; (2) Bu₃SnCl; (vii) NIS, CHCl₃/HOAc, rt; (viii) TBAF, THF, rt.

devices,⁵ such as organic light-emitting diodes (OLEDs),⁶ field-effect transistors (OFETs),⁷ photovoltaic devices (OPVs),⁸ photoconductive devices,⁹ and sensors.¹⁰ The optical and electronic properties of oligothiophenes and polythiophenes are very sensitive to conformation and morphology, and these properties can be modified chemically¹¹ through judicious structural variation. Until recently, relatively few types of branched or dendritic thiophene systems have been synthesized and investigated. Advincula and co-workers have synthesized rigid thiophene-based dendrimers that exhibited unique supramolecular assembling properties of potential interest in molecular electronics.¹² Because of their rigid structures, the optical and semiconducting properties of the conjugated dendrimers studied to date are primarily sensitive to intermolecular packing and are not subject to intramolecular interactions.¹³

In the present paper, we report on the synthesis and characterization of a series of dendrimers with oligothiophene arms connected by free rotating ester linkage cores. To improve the solubility and processability of our dendritic oligothiophene

systems, a hexyl substituent is introduced on every other thiophene unit in a pseudo “head-to-tail” coupled manner (analogous to those in highly regioregular head-to-tail coupled oligo- and poly-3-alkylthiophenes) with the aim of creating a perfectly regioregular microstructure in each arm. In addition, unlike the fully rigid thiophene-based dendrimers¹² discussed above, these macromolecules have labile morphology resulting in properties highly sensitive to solvent composition (solvation) and temperature changes. The oligothiophene arms can function both as the rigid scaffold and as the internal “reporters” of the dendrimer morphology. We also show how intramolecular interaction reversibly affects their optical and electrochemical behavior (solvatochromic and thermochromic properties) in dilute solutions.

Results and Discussion

Synthesis and Characterization. The synthetic approach used for various regioregular oligothiophenes (**2a–d**, **3a–c**) is outlined in Scheme 1. Palladium-catalyzed Stille reaction¹⁴ was employed for the cross-coupling of α -bromo- or α -iodothiophene with an appropriate thiophene organostannane to generate dimers and tetramers with moderate yields of around 50–70% after purification by silica gel flash chromatography. In the present work, using anhydrous DMF instead of toluene or THF as a solvent for the cross-coupling reactions gave a better yield and fewer side products. The *tert*-butyldimethylsilyl (TBS) protecting group installed on the 5-position of several oligothiophene intermediates (**2a**, **2b**, and **3a**), which served to achieve regioregularity in a pseudo “head-to-tail” coupled fashion, was found to be much more stable than a trimethylsilyl (TMS) protecting group. No desilylation was observed during the purification steps in the synthesis of these TBS-substituted intermediates. Tetrabutylammonium fluoride (TBAF) was used for the clean removal of the TBS protecting group, providing

(3) (a) Reetz, M. T.; Giebel, D. *Angew. Chem., Int. Ed.* **2000**, *39*, 2498–2501. (b) Boas, U.; Heegaard, P. M. H. *Chem. Soc. Rev.* **2004**, *33*, 43–63. (c) Ballauff, M.; Likos, C. N. *Angew. Chem., Int. Ed.* **2004**, *43*, 2998–3020.

(4) (a) Devadoss, C.; Bharathi, P.; Moore, J. S. *J. Am. Chem. Soc.* **1996**, *118*, 9635–9644. (b) Moore, J. S. *Acc. Chem. Res.* **1997**, *30*, 402–413. (c) Grayson, S. M.; Fréchet, J. M. J. *Chem. Rev.* **2001**, *101*, 3819–3868. (d) Peng, Z.; Pan, Y.; Xu, B.; Zhang, J. *J. Am. Chem. Soc.* **2000**, *122*, 6619–6623. (e) Berresheim, A. J.; Muller, M.; Mullen, K. *Chem. Rev.* **1999**, *99*, 1747–1786.

(5) Fichou, D., Ed. *Handbook of Oligo- and Polythiophenes*; Wiley: Weinheim, 1999.

(6) (a) Inganaes, O.; Berggren, M.; Andersson, M. R.; Gustafsson, G.; Hjertberg, T.; Wennerstroem, O.; Dyreklev, P.; Granstroem, M. *Synth. Met.* **1995**, *71*, 2121–2124. (b) Pei, J.; Yu, W.; Huang, W.; Heeger, A. J. *Macromolecules* **2000**, *33*, 2462–2471. (c) Mazzeo, M.; Vitale, V.; Della Sala, F.; Pisignano, D.; Anni, M.; Barbarella, G.; Favaretto, L.; Zanelli, A.; Cingolani, R.; Gigli, G. *Adv. Mater.* **2003**, *15*, 2060–2063.

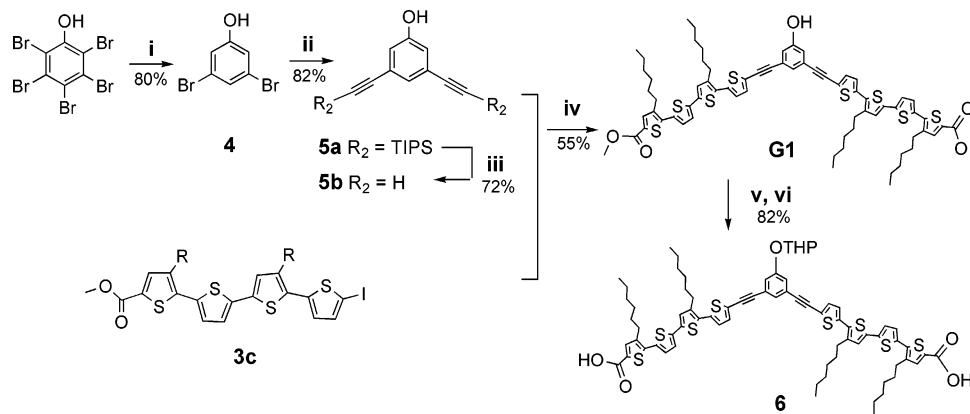
(7) (a) Koezuka, H.; Tsumura, A.; Ando, T. *Synth. Met.* **1987**, *18*, 699–704. (b) Katz, H. E.; Bao, Z.; Gilat, S. L. *Acc. Chem. Res.* **2001**, *34*, 359–369. (c) Salleo, A.; Chen, T. W.; Völkel, A. R.; Wu, Y.; Liu, P.; Ong, B. S.; Street, R. A. *Phys. Rev. B* **2004**, *70*, 115311.

(8) (a) Huynh, W. U.; Dittmer, J. J.; Alivisatos, A. P. *Science* **2002**, *295*, 2425–2427. (b) Padinger, F.; Rittberger, R. S.; Sariciftci, N. S. *Adv. Funct. Mater.* **2003**, *13*, 85–88. (c) Coakely, K. M.; Liu, Y.; McGehee, M. D.; Frindell, K. M.; Stucky, G. D. *Adv. Funct. Mater.* **2003**, *13*, 301–306.

(9) Yu, G.; Phillips, S. D.; Tomozawa, H.; Heeger, A. J. *Phys. Rev. B* **1990**, *42*, 3004.

(10) (a) Marsella, M. J.; Swager, T. M. *J. Am. Chem. Soc.* **1993**, *115*, 12214–12215. (b) McCullough, R. D.; Williams, S. P. *J. Am. Chem. Soc.* **1993**, *115*, 11608–11609. (c) Leclerc, M.; Ho, H. A. *J. Am. Chem. Soc.* **2004**, *126*, 1384–1387.

(11) Leclerc, M.; Ho, H. A. *Synlett* **2004**, *2*, 380–387. (12) (a) Xia, C.; Fan, X.; Locklin, J.; Advincula, R. C. *Org. Lett.* **2002**, *4*, 2067–2070. (b) Xia, C.; Fan, X.; Locklin, J.; Advincula, R. C.; Gies, A.; Nonidez, W. *J. Am. Chem. Soc.* **2004**, *126*, 8735–8743.

SCHEME 2. Synthetic Routes for G1 and Dendrimer Building Block 6^a

^a Reagents and conditions: (i) AlCl_3 , benzene, reflux; (ii) (triisopropylsilyl)acetylene, 3 mol % $\text{Pd}(\text{PPh}_3\text{CN})_2\text{Cl}_2$, 6 mol % $[(t\text{-Bu})_3\text{PH}]\text{BF}_4$, 2 mol % CuI , 2.5 equiv of $\text{HN}(i\text{-Pr})_2$, dioxane, rt; (iii) TBAF, THF, rt; (iv) 2 mol % $\text{Pd}(\text{PPh}_3)_2\text{Cl}_2$, 1 mol % CuI , Et_3N , reflux; (v) DHP, PPTS, CH_2Cl_2 , 40 °C; (vi) NaOH , $\text{EtOH}/\text{THF}/\text{H}_2\text{O}$, reflux.

quaterthiophene ester **3b** in 77% yield. It is worth mentioning that the introduction of methyl ester functionality at the terminal α -position facilitated chromatographic purification by increasing polarity and provided a useful scaffold from which to construct the dendrimers. Side products resulting from the homo-coupling of iodo-thiophene (around 20%) were always observed under these typical reaction conditions, and they could be readily isolated by silica gel chromatography. Nevertheless, this iterative synthetic strategy^{14b} could be repeated to provide hexamer, octamer, and other regioregular head-to-tail coupled oligothiophenes with longer conjugation length.

Scheme 2 describes the methods to synthesize **G1** and building block **6**. We chose 3,5-dibromophenol instead of 3,5-diiodophenol as the precursor of the core 3,5-diethynylphenol (**5b**) because the former was easier to synthesize, and we prepared it according to a literature procedure.^{15a} However, the palladium-mediated Sonogashira cross-coupling of 3,5-dibromophenol with (triisopropylsilyl)acetylene to obtain **5a** proved challenging. Typical workhorse palladium catalysts/ligands combination such as $\text{Pd}(\text{PPh}_3)_2\text{Cl}_2/\text{PPh}_3$, $\text{Pd}(\text{PPh}_3)_4$, or $\text{Pd}_2(\text{dba})_3/\text{PPh}_3$ all proved unsuccessful as they only generated monosubstituted instead of disubstituted product because of the reactivity difference between bromo- and iodo-substrates. Gratifyingly, the use of Fu's recipe consisting of $\text{Pd}(\text{PhCN})_2\text{Cl}_2$ and tri-*tert*-butylphosphonium tetrafluoroborate as reported in the literature^{15b} eventually provided the desired cross-coupled product and led to core **5b** (following a TBAF-induced desilylation) in an overall 59% yield over two steps. **G1** was also produced by palladium-catalyzed Sonogashira cross-coupling of iodo-substituted quaterthiophene **3c** with diethynyl core **5b**. Starting from **G1**, building block **6** was generated by hydrolyzing the tetrahydropyran (THP)-protected **G1** in good yield (82%). Higher generation dendrimers were prepared using an esterification

reaction between phenol functionality at the focal point of **Gn** and the dicarboxylic acid functional groups on the periphery of building block **6**.

The convergent assembly of dendrimers is outlined in Scheme 3. There were two main reasons for choosing esterification as the key reaction for building dendrimers. One is the poly(ester) dendrimer synthesis, which has been well developed, and efficient condensation reagents are available. Instead of using a rapid orthogonal coupling strategy,^{1d} we followed the traditional methodology of repeating coupling and activation steps enabling us to work under mild conditions, while retaining easy purification and good yield. Condensation reactions¹⁶ between oligothiophene carboxylic acid and phenol were used to furnish up to the third generation ester-linked thiophene dendrimers under neutral conditions. Furthermore, ester linkage provided the whole molecule with a mobile structure to adopt different conformations in response to environmental changes.

Dendrimers **G1–G3** are soluble in common organic solvents such as chloroform, tetrahydrofuran, chlorobenzene, and 1,2-dichlorobenzene. The singlet peak signal at 3.89 ppm in the ¹H NMR spectra of various ester-substituted intermediates and dendrimers can be assigned to the peripheral methyl ester protons, while the region of 2.7–2.8 ppm is assignable to the methylene protons on the hexyl side chain directly linked to thiophene rings for all intermediates and dendrimers. In **G1**, these two sets of signals have a ratio of 6:8, in **G2** 12:24, and in **G3** 24:56, consistent with the number of peripheral ester CH_3 protons and alkyl CH_2 protons, confirming the successful growth and structural uniformity of various dendrimers synthesized. In ¹³C NMR spectra, the diagnostic signals in the range of 80–95 ppm correspond to absorptions by alkyne carbons. In **G1**, there are only two types of alkyne carbons with an integrated ratio of 2:2, while in **G2** and **G3**, there are essentially four types of alkynyl carbons, and the ratios are 2:4:4:2 and 2:12:12:2, respectively, proportional to the number of expected alkynyl carbons in these molecules.

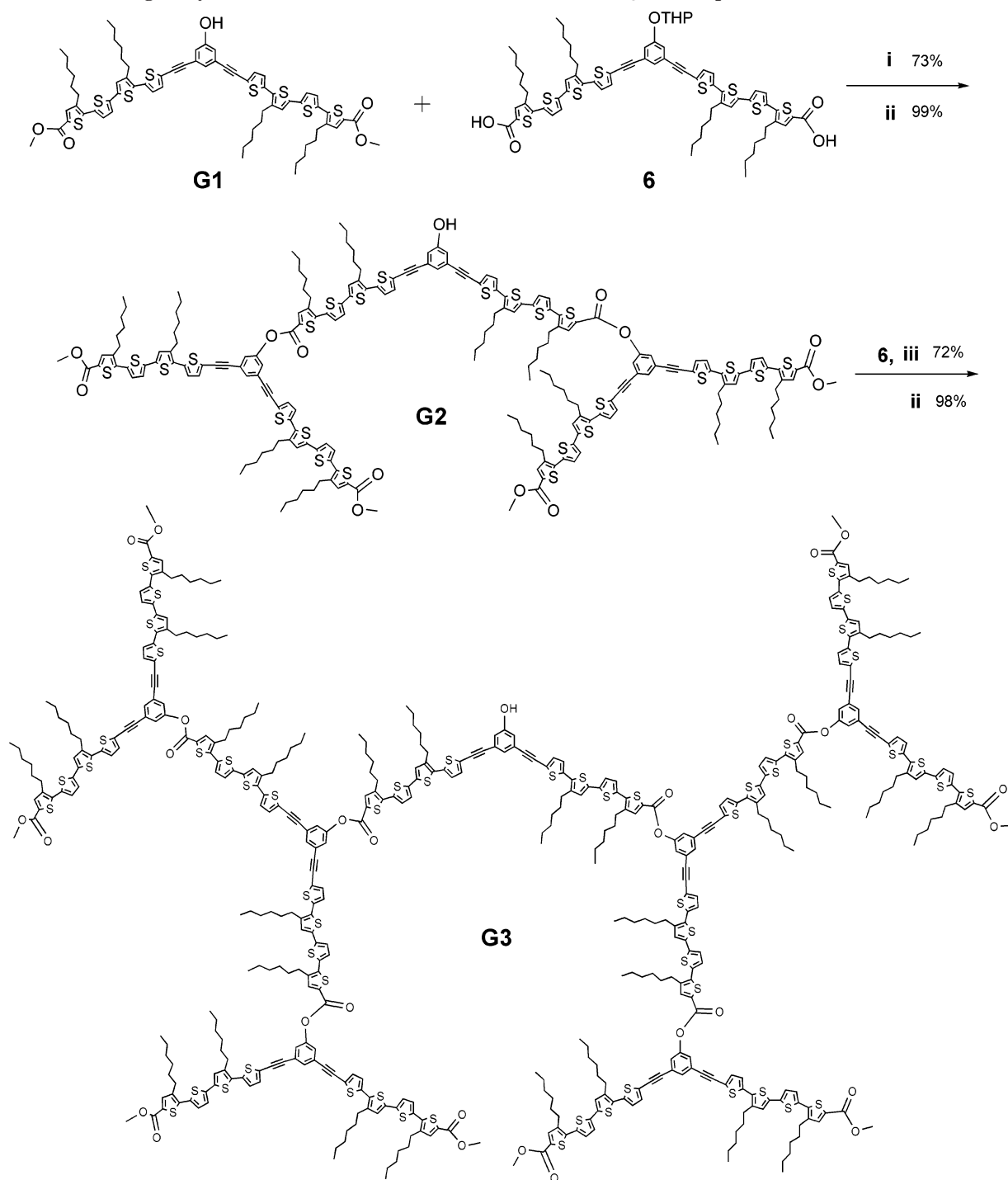
Photophysical Properties. Figure 1 shows the absorption spectra of dendrimers **G1**, **G2**, **G3**, and quaterthiophene **3b** in a dilute chloroform solution (good solvent) with the same

(13) For an interesting work on photochromic dendrimers containing an azobenzene linkage in the internal dendrimer structure that is capable of undergoing structural reorganization, see: Liao, L.-X.; Stellacci, F.; McGrath, D. V. *J. Am. Chem. Soc.* **2004**, *126*, 2181–2185.

(14) (a) Hassan, J.; Sevignon, M.; Gozzi, C.; Schulz, E.; Lemaire, M. *Chem. Rev.* **2002**, *102*, 1359–1469. (b) Ng, M.-K.; Wang, L.; Yu, L. *Chem. Mater.* **2000**, *12*, 2988–2995. (c) Zhao, C.; Zhang, Y.; Wang, C.; Rothberg, L. J.; Ng, M.-K. *Org. Lett.* **2006**, *8*, 1585–1588.

(15) (a) Lin, C.; Tour, J. J. *Org. Chem.* **2002**, *67*, 7761–7768. (b) Netherton, M. R.; Fu, G. C. *Org. Lett.* **2001**, *3*, 4295–4298.

(16) Messmore, B. W.; Hulvat, J. F.; Sone, E. D.; Stupp, S. I. *J. Am. Chem. Soc.* **2004**, *126*, 14452–14458.

SCHEME 3. Convergent Synthetic Routes for Dendrimers **G2** and **G3** with Quaterthiophene Arms^a

^a Reagents and conditions: (i) DIPC, DPTS, CH₂Cl₂, reflux; (ii) 3 M HCl, THF, 40 °C; (iii) DIPC, DPTS, CHCl₃, reflux.

concentration (4×10^{-6} M). Quaterthiophene **3b** has an absorption maximum at 395 nm with a molar extinction coefficient ϵ of 4.7×10^4 M⁻¹ cm⁻¹. It is noticed that **G1**'s absorption shows a moderate red shift ($\lambda_{\text{max}} = 415$ nm) relative to quaterthiophene **3b** due to a slight elongation in effective conjugation length upon coupling to a *meta*-linked phenyl bis-(acetylenic) unit. Given the "*meta*"-like relationship between the two quaterthiophene arms in **G1**, the effect of electronic delocalization due to cross-conjugation between the individual oligothiophene moieties is not expected to be significant. **G1**

has approximately doubled quaterthiophene **3b**'s molar extinction coefficient because it has two quaterthiophene moieties per molecule. On the contrary, both of the higher generation dendrimers **G2** and **G3** exhibit λ_{max} values at around 420 nm, only barely red-shifted by another 5 nm with respect to that of **G1**. Given the fact that the absorbance of higher generation **G3** is much greater than 1.0 at $c = 4 \times 10^{-6}$ M, additional spectroscopic measurements were performed on both **G2** and **G3** at different concentration regimes. It was unambiguously confirmed that λ_{max} and molar absorption coefficient values of

TABLE 1. Photophysical Properties of Quaterthiophene **3b** and Dendrimers **G1**, **G2**, **G3**

compound	$\lambda_{\max}^{\text{abs}}$ nm	$\lambda_{\max}^{\text{em}}$ nm	ϵ $\times 10^5 \text{ M}^{-1} \text{ cm}^{-1}$	ratio to ϵ of 3b	Φ_f^a	$\lambda_{\text{onset}}^{\text{abs}}$ nm	E_g^b eV
3b	395	523	0.47	1	13%	465	2.67
G1	415	521, 547	1.08	2.3	24%	486	2.55
G2	420	545	2.78	5.9	22%	491	2.53
G3	420	552	6.78	14.4	14%	494	2.51

^a Optical absorption and emission studies were performed in chloroform, and quantum yields were determined relative to Rhodamine 6G in methanol ($\Phi_f = 0.94$) as a standard.^{18a} Fluorescence quantum yield measurements were performed at concentrations where $A \leq 0.2$ for all compounds. Refractive index correction has been performed due to changing solvents. ^b Optical bandgaps E_g are estimated from onset absorption, which is 10% of the maximum absorption.^{18b}

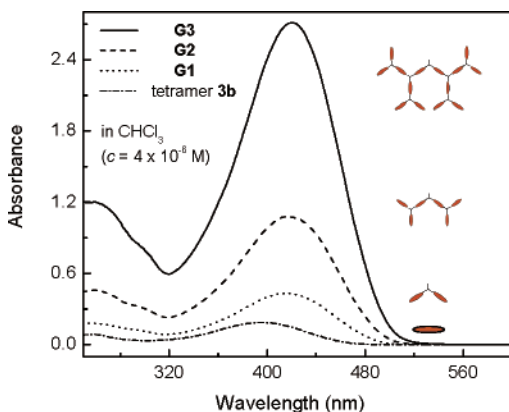


FIGURE 1. UV-vis absorption spectra of dendrimers **G1**, **G2**, **G3**, and quaterthiophene **3b** in chloroform ($c = 4 \times 10^{-6}$ M). Cartoon structures of dendrimers are also illustrated. The ellipses represent quaterthiophene arms, and short lines stand for the phenyl acetylene cores.

3b and all dendrimers are virtually independent of concentration changes (from 10^{-5} to 10^{-7} M) typically employed in spectroscopic studies (Supporting Information Figure S1). Overall, the molar extinction coefficients of various generations, within experimental error, are proportional to the number of quaterthiophene chromophores per dendrimer. On the basis of these optical absorption data, one can safely assume that the quaterthiophene moieties within each generation behave rather independently in dilute solutions as has been reported for other multichromophoric dendrimers in the recent literature.¹⁷

The basic photophysical data for **3b** and the dendrimers are summarized in the Table 1. The HOMO-LUMO gaps are estimated from the absorption onset where we arbitrarily choose an energy corresponding to where their extinction coefficients are at 10% of their maximum values. The quantum yields for fluorescence are determined to be 24%, 22%, and 14% for **G1**–**G3** in dilute chloroform solution, measured relative to Rhodamine 6G in methanol ($\Phi_f = 0.94$) as a standard.¹⁸ To minimize extensive fluorescence quenching due to intermolecular aggregations, all fluorescence quantum yield studies were carried out in fairly dilute solutions where absorbance values are less than 0.2, which typically correspond to $c = 10^{-6}$ – 10^{-7} M. The gradual reduction in quantum yields for dilute solutions of **G2** and **G3** suggests increasingly important intramolecular fluores-

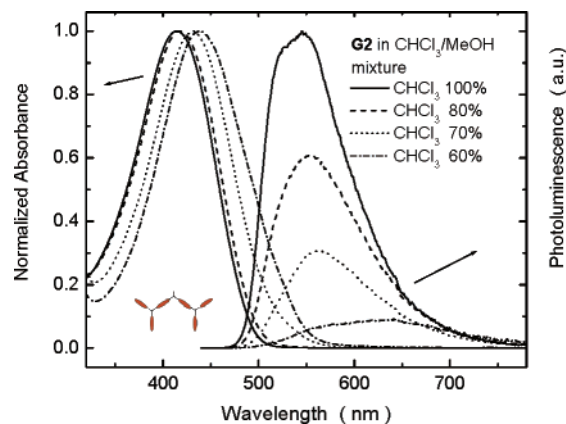


FIGURE 2. Optical absorption and emission spectra of **G2** in different mixtures of chloroform and methanol ($c = 1 \times 10^{-5}$ M).

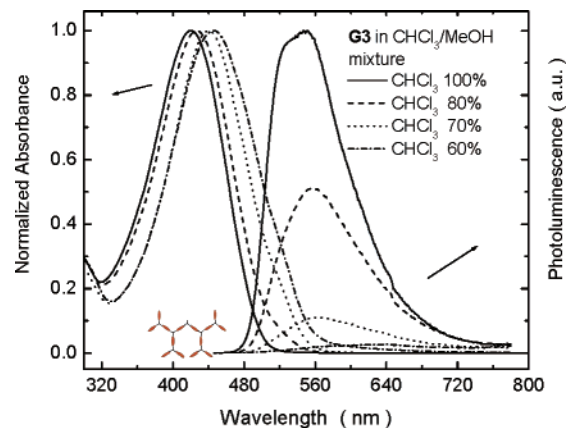


FIGURE 3. Optical absorption and emission spectra of **G3** in different mixtures of chloroform and methanol ($c = 2 \times 10^{-6}$ M).

cence quenching behavior is taking place as more quaterthiophene chromophore moieties are able to associate within the flexible dendrimer in higher generation. The ability of the chromophore units to aggregate internally, by virtue of the presence of various ester linkages, makes these dendrimers particularly sensitive to environmental conditions including solvent composition and temperature changes as discussed below.

Solvatochromism and Thermochromism. Notably, higher generation dendrimers **G2** and **G3** were found to show rather strong solvatochromic and thermochromic effects, in sharp contrast to **G1** and their linear oligomers. Figures 2 and 3 display the steady-state UV-vis absorption and emission spectra of **G2** and **G3** in a mixture of chloroform and methanol with different

(17) (a) Chen, J.; Li, S.; Zhang, L.; Liu, B.; Han, Y.; Yang, G.; Li, Y. *J. Am. Chem. Soc.* **2005**, *127*, 2165–2171. (b) Thomas, K. R. J.; Thompson, A. L.; Sivakumar, A. V.; Bardeen, C. J.; Thayumanavan, S. *J. Am. Chem. Soc.* **2005**, *127*, 373–383.

(18) (a) Jakubiak, R.; Bao, Z.; Rothberg, L. J. *Synth. Met.* **2000**, *114*, 61. (b) Tian, H.; Wang, J.; Shi, J.; Yan, D.; Wang, L.; Geng, Y.; Wang, F. *J. Mater. Chem.* **2005**, *15*, 3026–3033.

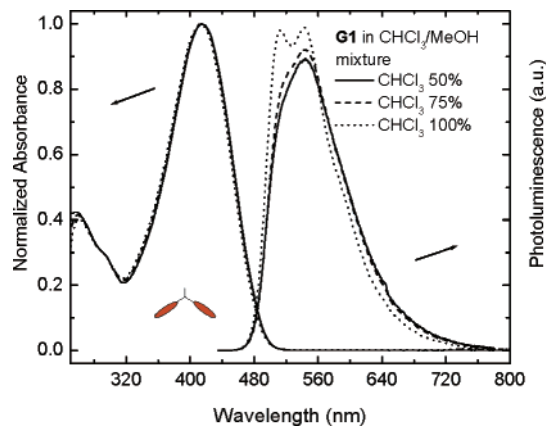


FIGURE 4. Optical absorption and emission spectra of **G1** in different mixtures of chloroform and methanol ($c = 1 \times 10^{-5}$ M).

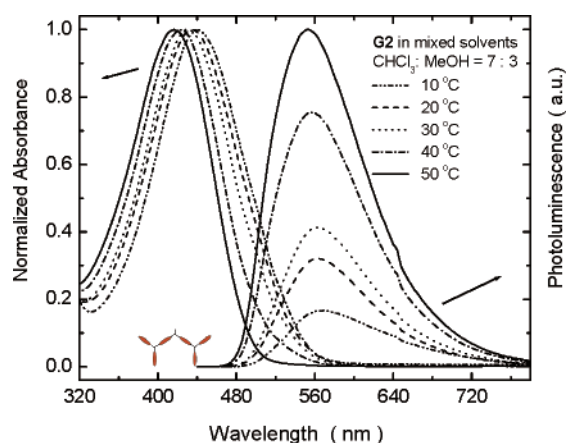


FIGURE 5. Temperature-dependent absorption and emission spectra of **G2** in a 70:30 mixture of chloroform and methanol ($c = 1 \times 10^{-5}$ M).

composition. Methanol is a poor solvent for the rigid oligothiophenes, and increasing its proportion in the solvent mixture results in an apparent red spectral shift to longer wavelength accompanied by a concomitant color change from yellow to red. The absorption maximum bathochromically shifts by 22 nm for **G2** and 27 nm for **G3** upon going from 100% chloroform to a mixture consisting of 60% chloroform and 40% methanol. No aggregation or precipitation was observed with increasing methanol content, and no further shifting of λ_{\max} values was observed after methanol is increased up to 40%. The fluorescence red-shifting is somewhat in line with those observed for the absorption, and the spectral change is accompanied by a continuous and dramatic reduction in the fluorescence quantum yield with increasing methanol content. In sharp contrast to both **G2** and **G3**, lower generation **G1** and linear quaterthiophene **3b** do not exhibit any observable solvatochromism under the same conditions. Figure 4 shows UV-vis absorption and emission spectra of **G1** in a similar mixture of chloroform and methanol. The fact that the spectral changes for both **G2** and **G3** occur in extremely dilute solutions ($\sim 10^{-5}$ – 10^{-7} M) and do not occur in **G1** or **3b** leads us to conclude that the spectral changes correspond to intramolecular interaction rather than intermolecular aggregation typical of conjugated polymers. Presumably, increasing the proportion of poor solvents such as

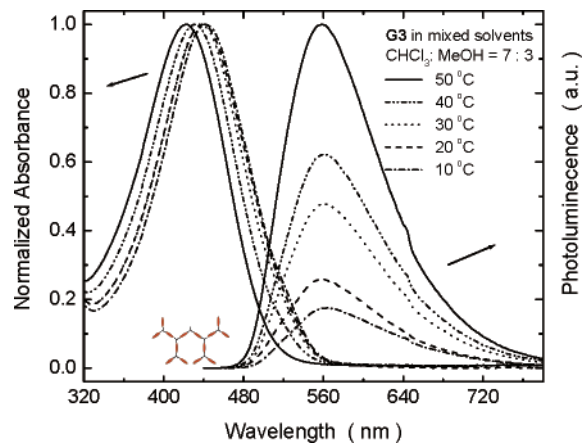


FIGURE 6. Temperature-dependent absorption and emission spectra of **G3** in a 70:30 mixture of chloroform and methanol ($c = 2 \times 10^{-6}$ M).

TABLE 2. Electrochemical Properties of Quaterthiophene **3b** and Dendrimers **G1**, **G2**, **G3**

compound	E_{pa} (eV) ^a	E_{pc} (eV) ^a	$E^{o'}$ (eV) ^a	$E_{1^{o'}}$ (eV) ^b	$E_{2^{o'}}$ (eV) ^b
3b	1.04	0.87	0.96		
G1	0.99	0.88	0.94	1.09 ^c	
G2	0.87	0.74	0.81	1.14	1.46
G3	0.84	0.68	0.76	1.16	1.46

^a Measured in a 4:1 v/v mixture of $\text{CHCl}_3/\text{CH}_3\text{CN}$ at room temperature. Anodic (E_{pa}), cathodic (E_{pc}), and half-wave potentials ($E^{o'} = (E_{pa} + E_{pc})/2$) are vs SCE (calibrated by Fc^+/Fc couple). ^b Dendrimer thin films coated on Pt wire working electrode and measured in CH_3CN at room temperature. Half-wave potentials ($E^{o'} = (E_{pa} + E_{pc})/2$) are vs SCE (calibrated by Fc^+/Fc couple). ^c Only E_{pa} could be observed for the film of **G1**.

methanol leads to a morphological change of the flexible dendrimer¹⁹ to a less mobile conformation where the thiophene units can interact among themselves more effectively. This type of intramolecular interaction is most pronounced in the higher generations (**G2** and **G3**), resulting in an improvement in effective conjugation length, which concomitantly red shifts their absorption and emission spectra (Figures 2 and 3). Intermolecular π - π stacking interactions and interchain excitations cause a concomitant reduction in fluorescence quantum yield, as has been demonstrated in analogous conjugated systems.^{20,21} Lower generation **G1** and quaterthiophene **3b** lack the internal ester core linkages and are therefore unable to reorganize intramolecularly to support strong interactions between quaterthiophene moieties and therefore do not exhibit any observable solvatochromic behavior under the same conditions.

To lend further support to our argument, reversible thermo-chromic behaviors were also observed in solutions of both **G2** and **G3**, changing their color from red to yellow with increasing temperature and reverting back to red when the temperature was lowered in a reversible manner. Figures 5 and 6 display the

(19) Likos, C. N.; Ballauff, M. *Top. Curr. Chem.* **2005**, *245*, 239–252.

(20) (a) Lévesque, I.; Leclerc, M. *Synth. Met.* **1997**, *84*, 203–204. (b) DiCésare, N.; Belletête, M.; Raymond, F.; Leclerc, M.; Durocher, G. *J. Phys. Chem. A* **1997**, *101*, 776–782. (c) DiCésare, N.; Belletête, M.; Leclerc, M.; Durocher, G. *Synth. Met.* **1998**, *98*, 31–40.

(21) (a) Collison, C. J.; Rothberg, L. J.; Treemaneekarn, V.; Li, Y. *Macromolecules* **2001**, *34*, 2346–2352. (b) Schenning, A. P. H. J.; Kilbinger, A. F. M.; Biscarini, F.; Cavallini, M.; Cooper, H. J.; Derrick, P. J.; Feast, W. J.; Lazzaroni, R.; Leclère, Ph.; McDonnell, L. A.; Meijer, E. W.; Meskers, S. C. J. *J. Am. Chem. Soc.* **2002**, *124*, 1269–1275.

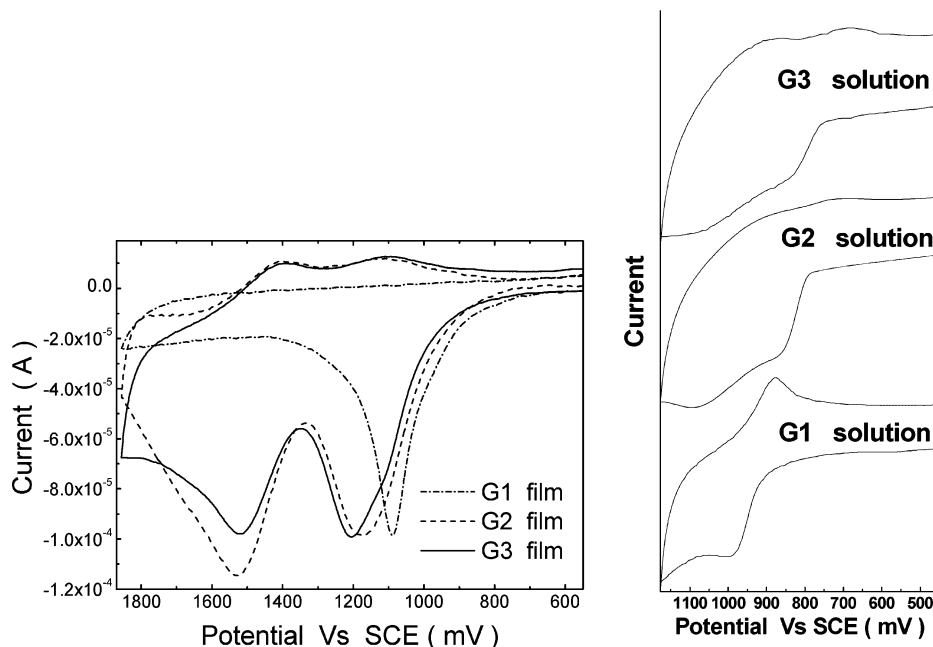


FIGURE 7. (Right) Cyclic voltammograms of **G1**, **G2**, and **G3** recorded in a 4:1 v/v mixture of $\text{CHCl}_3/\text{CH}_3\text{CN}$ containing TBAPF_6 (0.02 M) as electrolyte at room temperature. The scan rate was 100 mV/s. Potentials are reported versus SCE and calibrated by Fc/Fc^+ internal standard. Curves have been offset vertically for clarity. (Left) Cyclic voltammograms of **G1**, **G2**, and **G3** thin films deposited on Pt wire (1 mm diameter) electrodes recorded in CH_3CN containing TBAPF_6 (0.1 M) as electrolyte at room temperature. The scan rate was 100 mV/s. Potentials are reported versus SCE and calibrated by Fc/Fc^+ internal standard.

temperature dependence of the absorption and emission spectra of **G3** and **G2** in a 70/30 mixture of $\text{CHCl}_3/\text{MeOH}$. As indicated above, a solution of **G3** in this particular mixed solvent system exhibits an absorption maximum (λ_{max}) value of 440 nm at near room temperature (20 °C). Upon heating to 50 °C, the λ_{max} value was gradually blue-shifted by 20 nm, and, on the other hand, while being cooled to 10 °C, the λ_{max} was slightly red-shifted to 442 nm. It is also clear that at the same time the emission intensity of **G3** in solution is dramatically and continuously reduced along with decreasing temperature (Figure 6). This process is fully reversible and can be repeated many times in solution. Although essentially the same trend was observed for **G2** solution, no such thermochromic behavior could be observed for **G1** with any solvent composition within this temperature range (0–50 °C). The thin-film absorption spectra of these dendritic molecules have also been measured (Supporting Information Figure S2), and all dendrimers show essentially the same λ_{max} at 437 nm in the solid state, which are bathochromically shifted from their respective λ_{max} in chloroform. The overall effect of going from solution to solid state results in a presumably higher degree of aggregation of the oligothiophene units, analogous to what was observed in bad solvent systems as well as when the solutions were cooled below room temperature.

Electrochemical Properties. The redox behaviors of dendrimers **G1–G3** in solution and as thin films were investigated by cyclic voltammetry. All potentials have been calibrated with ferrocene/ferrocenium (Fc/Fc^+) couple as the internal standard and are reported versus saturated calomel electrode (SCE). The electrochemical data are summarized in Table 2. These dendritic materials demonstrate dramatic differences in both solid and solution states because of their different structures and morphologies. As shown in Figure 7, at room temperature in a 4:1 v/v mixture of $\text{CHCl}_3/\text{CH}_3\text{CN}$ ($c = 10^{-4}$ M), the quarter-

thiophene **3b** and dendrimers **G1–G3** showed quasi-reversible redox behavior with decreasing anodic half-wave potentials E_{p}^{a} at 0.96, 0.94, 0.81, and 0.76, respectively. These results are fully consistent with our optical absorption data, indicating a slight, if not significant, improvement in effective conjugation length as the generation increases.

Unlike the solution cases, the oligothiophene dendrimer thin films cast on Pt electrodes behave electrochemically differently in the -200 to 1500 mV range (vs SCE). While the film of **G1** shows only one anodic wave, those of **G2** and **G3** can undergo two successive oxidation processes due to the presence of a larger number of oligothiophene units. One also notices that there are significant increases of anodic potentials E_{pa} values from **G1** to **G2** (or **G3**), reflecting the fact that the compact conformations of higher generation dendrimers (**G2** and **G3**) are able to inhibit electrolyte diffusion from solution to the electrode surface. This observation indicates that the film morphology indeed plays an important role in their electrochemical behavior.

In summary, we have designed and synthesized a new type of dendrimer with oligothiophene arms up to the third generation. The synthetic strategy is highly repetitive and includes Stille cross-coupling reactions for oligothiophenes, Sonogashira cross-coupling reactions for building blocks, and esterification reactions for the dendrimer assembly. The optical and electrochemical properties of these series of dendrimers are found to be strongly influenced by their morphologies. The systematic incorporation of rigid oligothiophene arms to shape non-consistent ester-linked dendrimers causes higher generation ones (**G2** and **G3**) to exhibit thermochromism and solvatochromism even though their oligomeric counterpart (**3b**) and lower generation (**G1**) analogue do not. Their interesting solvatochromic and thermochromic behaviors are comparable to those of typical oligo- and polythiophenes. These structurally well-

defined molecules are currently studied at the molecular level by immobilization of the various dendritic molecules as monolayers on glass surface, to gain a better understanding of the mechanism responsible for the spectral changes in different morphological states.

Experimental Section

Synthesis of Oligothiophenes. Scheme 1 shows the synthetic routes for the oligothiophene monomer, dimers, and tetramers. Compounds **1a**, **1b**, **2b**, **2d**, **3a**, 2-(*tert*-butyldimethylsilyl)-5-(tributylstannyl)thiophene, and 2-(tributylstannyl)thiophene were prepared according to literature procedures.¹⁴ Typical synthetic procedures for the Stille cross-coupling reaction used to create dimers and tetramers are provided in the Supporting Information. Desilylated quaterthiophene **3b** (X = H) was purified by flash chromatography over silica gel to afford a bright orange-yellow solid. ¹H NMR (CDCl₃, δ ppm): 0.89 (6H, t), 1.31–1.39 (12H, br), 1.69 (4H, m), 2.76 (4H, m), 3.89 (3H, s), 7.04 (1H, s), 7.08 (1H, t), 7.12 (2H, s), 7.15 (1H, d), 7.33 (1H, d), 7.63 (1H, s). ¹³C NMR (CDCl₃, δ ppm): 14.0, 22.5, 22.6, 29.1, 29.2, 29.3, 29.4, 30.2, 30.5, 31.5, 31.6, 52.1, 123.8, 124.0, 125.4, 125.9, 126.7, 127.4, 127.5, 129.9, 130.2, 133.7, 134.2, 135.7, 136.1, 137.7, 138.2, 139.9, 140.4, 162.5. HRMS (ESI) *m/z* calcd for C₃₀H₃₇O₂S₄ (M + H⁺), 557.1671; found, 557.1655.

Synthesis of Dendrimer G1 and Building Block 6. Scheme 2 shows the synthetic routes for the core **G1** and building block **6**. Compounds **4**, **5a**, and **5b** were prepared according to literature procedures.¹⁵

G1. A mixture of iodo-quaterthiophene **3c** (4.14 g, 6.06 mmol), compound **5b** (0.358 g, 2.52 mmol), copper(I) iodide (0.0048 g, 0.0252 mmol, 1 mol %), Pd(PPh₃)₂Cl₂ (0.035 g, 0.0504 mmol, 2 mol %), and triethylamine (80 mL) was stirred at 70 °C under nitrogen for 20 h. After the reaction was completed, the mixture was slowly poured into HCl (80 mL, 3 M), cooled in an ice–water bath, and then extracted with dichloromethane. The organic phase was washed with deionized water and brine, dried over anhydrous sodium sulfate, and concentrated under vacuum. The residue was further purified by flash chromatography on silica gel (eluting with CH₂Cl₂/hexane from 1:1 ratio to pure CH₂Cl₂) to provide **G1** as an orange-yellow powder in 55% yield. ¹H NMR (CDCl₃, δ ppm): 0.91 (12H, br), 1.30–1.42 (24H, br), 1.65–1.68 (8H, br), 2.77 (8H, m), 3.89 (6H, s), 5.03 (1H, s), 6.98 (2H, s), 7.05 (4H, m), 7.12 (2H, d), 7.13 (2H, d), 7.23 (2H, d), 7.30 (1H, s), 7.63 (2H, s). ¹³C NMR (CDCl₃, δ ppm): 14.0, 22.5, 22.6, 29.1, 29.2, 29.4, 29.6, 30.3, 30.4, 31.6, 31.7, 52.1, 83.3, 93.3, 118.4, 122.7, 124.2, 124.6, 125.7, 127.1, 127.2, 127.7, 129.7, 130.4, 132.7, 134.3, 135.0, 136.1, 137.7, 137.9, 138.1, 140.3, 141.3, 155.5, 162.6. HRMS (MALDI-TOF) calcd for C₇₀H₇₃O₅S₈⁺, 1250.8746; found, 1251.0809.

Building Block 6. A mixture of **G1** (0.35 g, 0.28 mmol), 3,4-dihydro-2H-pyran (0.071 g, 0.85 mmol), and pyridinium *p*-toluenesulfonate (0.0014 g, 0.0056 mmol, 2 mol %) in dichloromethane (20 mL) was stirred at 40 °C under nitrogen for 12 h. The resulting mixture was washed with deionized water, extracted with dichloromethane, dried over anhydrous sodium sulfate, and concentrated under vacuum. The residue was further purified by flash chromatography on silica gel (eluting with CH₂Cl₂/hexane from 1:1 ratio to 3:1) to provide THP-protected **G1** as orange-red flakes (0.36 g, 98%). ¹H NMR (CDCl₃, δ ppm): 0.91 (12H, br), 1.30–1.42 (24H, br), 1.62–1.71 (10H, br), 1.89 (2H, m), 1.98 (2H, m), 2.75–2.79 (8H, m), 3.68 (2H, t), 3.89 (6H, s), 5.48 (1H, t), 7.05 (4H, m), 7.13 (4H, dd), 7.20 (2H, d), 7.23 (2H, d), 7.33 (1H, s), 7.63 (2H, s). ¹³C NMR (CDCl₃, δ ppm): 14.0, 18.5, 22.5, 22.6, 25.1, 28.9, 29.0, 29.2, 29.3, 29.6, 30.2, 30.4, 31.6, 31.7, 52.1, 61.9, 83.0, 93.6, 96.4, 119.5, 122.6, 124.1, 125.5, 127.0, 127.5, 127.6, 129.6, 130.1, 132.6, 134.1, 134.8, 136.1, 137.66, 137.69, 138.0, 140.1, 141.1, 156.8, 162.5. For the subsequent basic hydrolysis reaction, ethanol (10 mL), deionized water (5 mL), and sodium

hydroxide (0.029 g, 0.74 mmol) were added to a solution of the resulting **G1** in THF (10 mL), and the mixture was refluxed for 2 h. The solvent was removed under vacuum, and the residue was acidified with acetic acid and extracted with ethyl acetate. The organic phase was washed with DI water, dried over anhydrous sodium sulfate, and solvent was removed in vacuo. The residue was further dried in a vacuum oven to afford building block **6** (0.32 g, 82% over two steps) as a red powder. ¹H NMR (*d*₆-DMSO, δ ppm): 0.86 (12H, br), 1.21–1.42 (24H, br), 1.52–1.70 (12H, br), 1.80 (2H, m), 2.75 (8H, t), 3.68 (2H, t), 5.61 (1H, t), 7.23 (4H, m), 7.28 (2H, d), 7.33 (2H, s), 7.35 (1H, s), 7.37 (2H, d), 7.45 (2H, d), 7.56 (2H, s). ¹³C NMR (*d*₆-DMSO, δ ppm): 13.4, 18.0, 21.57, 21.59, 24.3, 28.0, 28.1, 28.3, 28.6, 29.2, 29.3, 29.4, 30.5, 30.6, 61.3, 82.7, 93.0, 95.9, 119.4, 121.1, 123.2, 124.7, 125.9, 126.7, 127.3, 127.8, 132.6, 128.3, 133.4, 134.0, 135.3, 135.6, 136.9, 139.8, 141.1, 156.4, 162.1.

Synthesis of Dendrimers G2 and G3. Scheme 3 shows the synthetic approach to making various generation dendrimers. A synthetic procedure for **G2** derived from the literature¹⁶ is described as follows: To a mixture of building block **6** (0.144 g, 0.11 mmol), **G1** (0.317 g, 0.25 mmol), and DPTS (0.312 g, 1 mmol) in dichloromethane (40 mL) was added 1,3-diisopropylcarbodiimide (0.126 g, 1 mmol), and the reaction mixture was heated at reflux for 24 h. Upon cooling to room temperature, the precipitate was filtered and washed with CH₂Cl₂ to afford a red powder (0.30 g, 0.08 mmol). The crude solid was redissolved in THF (10 mL) and treated with a few drops of HCl (3 M), and stirred for 5 h. The solvent was removed under vacuum, and the residue was further purified by flash chromatography on silica gel (eluting with chloroform/diethyl ether from 200:1 ratio to 100:1) to provide **G2** (0.292 g, 0.079 mmol, 72% over two steps) as a red solid. ¹H NMR (CDCl₃, δ ppm): 0.91 (36H, br), 1.33–1.44 (72H, br), 1.65–1.75 (24H, br), 2.76 (20H, t), 2.85 (4H, t), 3.88 (12H, s), 6.98 (2H, s), 7.05 (12H, m), 7.11 (4H, d), 7.13 (4H, d), 7.15 (2H, d), 7.18 (2H, d), 7.12–7.25 (6H, m), 7.28 (1H, s), 7.40 (4H, s), 7.58 (2H, s), 7.63 (4H, s), 7.82 (2H, s). ¹³C NMR (CDCl₃, δ ppm): 14.0, 22.6, 22.7, 29.1, 29.2, 29.3, 29.4, 29.5, 29.7, 30.3, 30.5, 31.6, 31.7, 52.1, 83.0, 84.3, 92.8, 93.7, 119.5, 122.2, 122.7, 124.1, 124.3, 124.6, 125.5, 126.1, 127.0, 127.1, 127.6, 127.9, 128.5, 128.8, 129.6, 129.9, 130.1, 131.4, 132.7, 132.9, 133.8, 134.1, 134.7, 134.9, 136.2, 137.5, 137.7, 138.0, 138.1, 138.5, 139.6, 140.1, 140.4, 141.1, 141.2, 150.4, 156.8, 159.8, 162.5. MALDI-TOF calcd for C₂₀₈H₂₁₄O₁₃S₂₄⁺, 3690.48; found, 3690.22. Anal. Calcd for C₂₀₈H₂₁₄O₁₃S₂₄: C, 67.68; H, 5.84. Found: C, 67.48; H, 5.68.

A similar procedure was used to prepare **G3**, also isolated as a red solid, which was further purified by flash chromatography on silica gel (eluting with chlorobenzene/THF from 200:1 ratio to 50:1), yield 70% for two steps. ¹H NMR (CDCl₃, δ ppm): 0.90–0.92 (84H, br), 1.33–1.44 (168H, br), 1.66–1.76 (56H, br), 2.79 (44H, t), 2.85 (12H, t), 3.89 (24H, s), 6.99 (4H, s), 7.05–7.07 (28H, br), 7.11 (16H, d), 7.17 (12H, dd), 7.23–7.25 (14H, dd), 7.28 (2H, s), 7.40 (10H, s), 7.57 (5H, s), 7.62 (8H, s), 7.82 (6H, s). ¹³C NMR (CDCl₃, δ ppm): 14.0, 22.5, 22.6, 29.1, 29.2, 29.4, 29.5, 29.6, 30.3, 30.4, 31.6, 31.7, 52.0, 83.2, 84.3, 92.8, 93.5, 118.6, 122.5, 122.6, 122.9, 124.2, 124.3, 124.4, 124.5, 124.7, 125.7, 127.0, 127.2, 127.7, 128.1, 128.9, 129.7, 129.9, 130.0, 130.5, 131.5, 132.7, 132.9, 133.9, 134.3, 134.9, 135.0, 135.1, 136.1, 137.6, 137.7, 137.8, 138.1, 138.2, 138.6, 139.6, 140.3, 140.6, 141.3, 141.4, 150.6, 155.9, 159.8, 162.5. MALDI-TOF for (C₄₈₄H₄₉₃O₂₉S₅₆ + Na)⁺ calcd, 8582.15; found, 8582.49. Anal. Calcd for C₄₈₄H₄₉₄O₂₉S₅₆: C, 67.83; H, 5.81. Found: C, 67.61; H, 5.98.

Acknowledgment. We gratefully acknowledge financial support by the University of Rochester, the American Chemical Society PRF Type G (#43328-G7), and the New York State Office of Science, Technology, and Academic Research (#C050045). Mass spectrometry was provided by the Washington University Mass Spectrometry Resource with support from the NIH National Center for Research Resources (Grant No. P41RR0954).

M.-K.N. thanks the NYSTAR James D. Watson Investigator Program (2005). L.J.R. wishes to thank the National Science Foundation (award number DMR0513416). O.H. is the recipient of a summer fellowship through the NSF-REU program (2004). We thank Prof. J. P. Dinnocenzo for helpful discussions.

Supporting Information Available: Detailed experimental procedures for the synthesis and characterization of dendrimers and intermediates. This material is available free of charge via the Internet at <http://pubs.acs.org>.

JO0619581